THE ASTROPHYSICAL JOURNAL, 538:L129–L132, 2000 August 1

THE ENIGMATIC RADIO AFTERGLOW OF GRB 991216

D. A. FRAIL,[1] E. BERGER,[2] T. GALAMA,[2] S. R. KULKARNI,[2] G. H. MORIARTY-SCHIEVEN,[3]
G. G. POOLEY,[4] R. SARI,[5] D. S. SHEPHERD,[1] G. B. TAYLOR,[1] AND F. WALTER[2]
Received 2000 March 16; accepted 2000 June 19; published 2000 July 28

ABSTRACT

We present broadband radio observations spanning 1.4–350 GHz of the afterglow of GRB 991216, taken 1–80 days after the burst. The optical and X-ray afterglow of this burst were fairly typical and are explained by a jet fireball. In contrast, the radio afterglow is unusual in two respects: (1) the radio light curve does not show the usual rise to maximum flux on timescales of weeks and instead appears to be declining already on day 1; and (2) the power-law indices show significant steepening from the radio through the X-ray bands. We show that the standard fireball model, in which the afterglow is from a forward shock, is unable to account for point 1, and we conclude that the bulk of the radio emission must arise from a different source. We consider two models, neither of which can be ruled out with the existing data. In the first (conventional) model, the early radio emission is attributed to emission from the reverse shock, as in the case of GRB 990123. In the second "dual fireball" model, the radio emission originates from the forward shock of an isotropically energetic fireball (10^{54} ergs) expanding into a tenuous medium (10^{-4} cm^{-3}), while the optical and X-ray emission originate in a jetlike outflow. Finally, we note that the near-IR bump of the afterglow is similar to that seen in GRB 971214, and no fireball model can explain this bump.

Subject headings: cosmology: observations — gamma rays: bursts — radio continuum: general

1. INTRODUCTION

The intense gamma-ray burst GRB 991216 was detected on 1999 December 16.67 UT by the Burst and Transient Source Experiment (BATSE) on board the *Compton Gamma Ray Observatory* satellite (Kippen, Preece, & Giblin 1999). Follow-up observations with the positional counter array (PCA) instrument on the *Rossi X-Ray Timing Explorer* (*RXTE*) satellite resulted in the detection of a previously uncataloged X-ray source, which was subsequently seen to fade by a factor of 5, 7 hours later (Takeshima et al. 1999). Uglesich et al. (1999) identified a fading optical source at a position consistent with the *RXTE* transient, and shortly thereafter the radio counterpart was discovered (Taylor & Berger 1999). Vreeswijk et al. (1999) derive a lower limit of $z > 1.02$ based on a system of Fe II, Mg II, and Mg I absorption lines.

Here we present radio measurements of this burst from 1 to 350 GHz. While the emission from X-ray and optical afterglow was fairly typical (Halpern et al. 2000), the radio afterglow of GRB 991216 was unusual in two respects. First, the onset of the decay began much earlier (<1.5 days) than that in most radio afterglows (10–100 days). Second, the temporal decay indices in the radio, optical, and X-ray bands are markedly different from each other. We explore a number of possible explanations for this behavior.

2. OBSERVATIONS AND RESULTS

Very Large Array (*VLA*).[6]—A log of the observations and flux density measurements are summarized in Table 1. We used J0509+1011 (at 8.46 and 4.86 GHz) and J0530+135 (at 1.43 GHz) for phase calibration. J0542+498 was used for flux calibration at all frequencies.

Very Long Baseline Array (*VLBA*).[6]—A single 2 hr observation was carried out at 8.42 GHz, and 2 bit samples of a 64 MHz bandwidth signal in one hand of polarization were recorded. The nearby (<1°.1) calibrator J0509+1011, a core jet source, was observed every 3 minutes for delay, fringe rate, and fringe phase calibration. The radio afterglow was detected at a position of (epoch J2000) $\alpha = 5^{h}9^{m}31^{s}.2983$, $\delta = +11°17'7''.262$ (with 1 σ error of 0″.001 in each coordinate). The source is unresolved with a size of less than 0″.001.

Ryle Telescope.—Observations at 15 GHz with the Ryle Telescope at Cambridge (UK) were made by interleaving 15 minute scans of GRB 991216 with short scans of the phase calibrator J0509+1011. The flux density scale was tied to observations of 3C 48 and 3C 286. The source was detected only on the first epoch.

Owens Valley Radio Observatory (*OVRO*) *Interferometer*.—The source was observed for a single 13 hr track in two continuum 1 GHz bands (central frequencies 98.481 and 101.481 GHz) under good 3 mm weather conditions. Gain calibration used the quasar 0528+134, while observations of Uranus and 3C 454.3 provided the flux density calibration scale with an estimated uncertainty of ~20%. See Shepherd et al. (1998) for details of the calibration and imaging. No source was detected.

James Clark Maxwell Telescope (*JCMT*).[7]—Observations in the 350 GHz band were made using the Submillimeter Common-User Bolometer Array (Holland et al. 1999). The data were taken under good sky conditions on both nights. For flux calibration we used the source CRL 618 and assumed its flux density to be 4.57 ± 0.21 Jy. The pointing was monitored and found to vary by less than 2″. See Kulkarni et al. (1999) for

[1] National Radio Astronomy Observatory, P.O. Box O, Socorro, NM 87801.
[2] California Institute of Technology, Owens Valley Radio Observatory 105-24, Pasadena, CA 91125.
[3] Joint Astronomy Centre, 600 North Aohoku Place, Hilo, HI 96720.
[4] Mullard Radio Astronomy Observatory, Cavendish Laboratory, Madingley Road, Cambridge CB3 0HE, England, UK.
[5] California Institute of Technology, Theoretical Astrophysics 130-33, Pasadena, CA 91125.
[6] The NRAO is a facility of the National Science Foundation operated under cooperative agreement by Associated Universities, Inc. NRAO operates both the VLA and the VLBA.

[7] The JCMT is operated by The Joint Astronomy Centre on behalf of the Particle Physics and Astronomy Research Council of the UK, the Netherlands Organization for Scientific Research, and the National Research Council of Canada.

TABLE 1
RADIO OBSERVATIONS OF GRB 991216

Epoch (UT) (1)	Δt (days) (2)	Telescope (3)	ν_o (GHz) (4)	$S \pm \sigma$ (μJy) (5)
1999 Dec 18.00	1.33	Ryle	15.0	1100 ± 250
1999 Dec 18.16	1.49	VLA	8.46	960 ± 67
1999 Dec 18.32	1.65	VLBA	8.42	705 ± 85
1999 Dec 18.48	1.81	JCMT	350	650 ± 1560
1999 Dec 19.30	2.63	OVRO	99.9	90 ± 700
1999 Dec 19.35	2.68	VLA	8.46	607 ± 32
1999 Dec 19.45	2.78	JCMT	350	−2000 ± 1670
1999 Dec 20.09	3.42	Ryle	15.0	−100 ± 400
1999 Dec 22.01	5.34	Ryle	15.0	−10 ± 200
1999 Dec 23.30	6.63	VLA	8.46	343 ± 43
1999 Dec 24.29	7.62	VLA	8.46	127 ± 58
1999 Dec 26.40	9.73	VLA	8.46	170 ± 72
1999 Dec 28.24	11.57	VLA	8.46	211 ± 25
1999 Dec 29.43	12.76	VLA	8.46	136 ± 37
1999 Dec 31.26	14.59	VLA	8.46	123 ± 39
2000 Jan 02.01	16.34	VLA	8.46	130 ± 22
2000 Jan 03.11	17.44	VLA	8.46	131 ± 36
2000 Jan 03.11	17.44	VLA	4.86	126 ± 31
2000 Jan 03.11	17.44	VLA	1.43	257 ± 100
2000 Jan 06.15	20.48	VLA	8.46	123 ± 30
2000 Jan 23.95	38.28	VLA	8.46	79 ± 31
2000 Jan 28.16	42.49	VLA	8.46	148 ± 33
2000 Feb 05.18	50.51	VLA	8.46	3.1 ± 30
2000 Feb 15.07	60.40	VLA	1.43	−55 ± 37
2000 Feb 15.07	60.40	VLA	8.46	9.6 ± 24
2000 Mar 03.85	78.18	VLA	8.46	47.0 ± 19

NOTE.—Col. (1): UT date of the start of each observation. Col. (2): Time elapsed since the GRB 991216 event (i.e., t_0 = 1999 December 16.67 UT). Col. (3): Telescope name. Col. (4): Observing frequency. Col. (5): Flux density of the radio transient, with the error given as the rms noise on the image. The epoch on 1999 January 23.95 UT is an average of 2 days of data (January 21.95 and January 25.94 UT). All VLA observations were obtained in the B-array configuration.

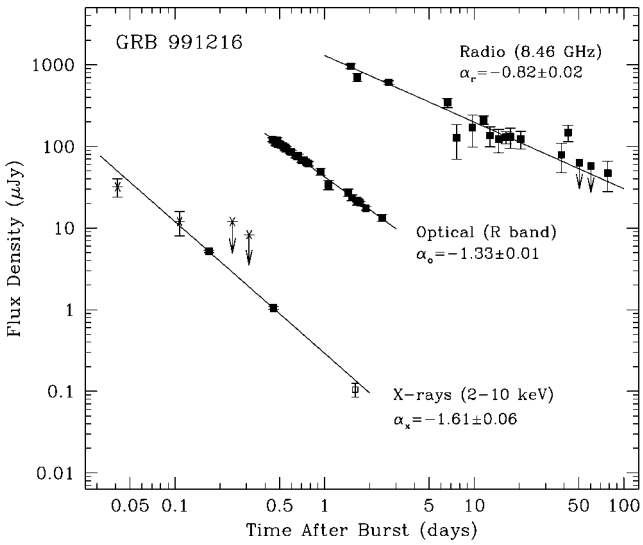

FIG. 1.—Broadband light curves of GRB 991216. Upper limits are plotted as the peak flux density at the location of the afterglow plus 2 times the rms noise in the image. The *R*-band data are taken from Halpern et al. (2000). Optical magnitudes were converted to Jy flux units (Fukugita, Shimasaku, & Ichikawa 1995), but no correction has been made for Galactic extinction. The X-ray data are measurements taken by the all-sky monitor (*asterisks*) and the PCA (*filled squares*) instruments on *RXTE* (Corbet & Smith 1999; Takeshima et al. 1999) and the *Chandra X-Ray Observatory* (*open square*; Piro et al. 1999). X-ray fluxes are converted to Jy using the X-ray slope $\beta_X = -1.1$ derived by Takeshima et al. (1999). The solid lines are noise-weighted least-squares fits to the data, with the slopes α_ν as indicated (see text for details).

details of data reduction. The source was not detected at either epoch. At the position of GRB 991216 we derive an average flux of -0.28 ± 1.1 mJy.

In Figure 1 we display the 8.46 GHz light curve, as well as the X-ray and optical (*R*-band) light curves obtained from measurements reported in the GRB Coordinates Network (GCN)[8] and Halpern et al. (2000). A noise-weighted least-squares fit of the form $F_\nu \propto t^{\alpha_\nu}$ was made to each of these light curves. Using all of the 8.46 GHz data, including the upper limits, we derive $\alpha_r = -0.82 \pm 0.02$ ($\chi^2_r = 26.5/15$; here χ^2_r is the reduced χ^2). A similar least-squares fit of the optical and X-ray data over the first 3 days (Fig. 1) yields $\alpha_o = -1.33 \pm 0.01$ ($\chi^2_r = 11/28$) and $\alpha_X = -1.61 \pm 0.06$ ($\chi^2_r = 7.7/3$).

3. THE FAILURE OF THE BASIC AFTERGLOW MODEL

The radio afterglow from GRB 991216 is unusual on two counts. First, the radio afterglow in the centimeter band does not show the usual rise to a peak value f_m (at epoch t_m) before undergoing a power-law decay. The radio flux appears to decline continuously starting from the epoch of the first observation. Thus, $t_m < 1.49$ days as compared to the 10–100 days seen in other bursts (e.g., Frail, Waxman, & Kulkarni 2000). Second, the temporal decay indices (α_ν) in the radio, optical, and X-ray bands are markedly different from each other. Proceeding from radio to higher frequencies, α_ν steepens by ~0.4 every four decades in frequency.

[8] Available at http://lheawww.gsfc.nasa.gov/docs/gamcosray/legr/bacodine/gcn_main.html.

In contrast, the optical and X-ray afterglow appears to find a straightforward explanation in the standard afterglow model in which a jet geometry is invoked (Halpern et al. 2000). Below we show that the radio observations cannot be reconciled with a standard jet (or sphere) afterglow model. We explore possible modifications to the standard model.

The simplest afterglow model is one in which the broadband afterglow emission arises from the forward shock of a relativistic blast wave propagating into a constant density medium (Sari, Piran, & Narayan 1998). It is assumed that the electrons in the forward shock region are accelerated to a power-law distribution for $\gamma_e > \gamma_m$, $dN/d\gamma_e \propto \gamma_e^{-p}$; here γ_e is the Lorentz factor of the electrons, p is the power-law index and γ_m is the minimum Lorentz factor. Gyration of these electrons in strong postshocked magnetic fields gives rise to broadband afterglow emission. Two modifications to this picture are routinely considered: (1) an inhomogeneous circumburst medium (specifically, $\rho(r) \propto r^{-2}$; here ρ is the density at distance r from the source)—such a circumburst medium is expected should GRBs originate from massive stars (Chevalier & Li 1999); and (2) a jetlike geometry for the blast wave (Rhoads 1997; Sari, Piran, & Halpern 1999).

Regardless of these modifications, the broadband spectrum is composed of three characteristic frequencies: ν_a, the synchrotron self-absorption frequency; ν_m, the frequency at which the emission peaks (and attributed to the electrons with Lorentz factor γ_m); and ν_c, the cooling frequency. Electrons radiating photons with frequency greater than ν_c cool on timescales faster than the age of the blast wave. The evolution of these fre-

quencies is determined by the dynamics of the blast wave. The usual ordering of these frequencies at epochs relevant to the discussion here is $\nu_a < \nu_m < \nu_c$.

For GRB 991216 the early radio decay implies that ν_m is already below the centimeter radio band at 1.49 days. The steepening of the afterglow emission from optical to X-ray can be explained by placing ν_c between the optical and X-ray bands. The expected steeping $\Delta\alpha$ is $\frac{1}{4}$, which is consistent with $\alpha_o - \alpha_X = 0.28 \pm 0.06$. However, we are unable to explain the decay in the radio band, since no additional steepening is expected between ν_m and ν_c.

The standard afterglow model can be made to agree with the light curves by postulating an energy slope p, which gradually steepens with increasing electron energy γ_e. Nonetheless, the invocation of curvature in the energy distribution of the electrons cannot explain the observed broadband spectrum (Fig. 2) of the afterglow on December 18 (corresponding to 1.33 days after the burst). A plausible fit to the entire data is obtained for $p = 2.2$ with $\nu_a = 1.3$ GHz, $\nu_m = 270$ GHz, $\nu_c = 7 \times 10^{16}$ Hz, and $f_m = 3.4$ mJy; this fit is displayed by the dashed line in Figure 2. As the blast wave slows down, ν_m moves to lower values while preserving f_m, and thus we expect the flux in the centimeter band to rise, whereas the observed flux falls. If the afterglow has a jetlike geometry, then the radio afterglow is expected to rise until the epoch t_j and subsequently decay very slowly ($f_\nu \propto t^{-1/3}$) until ν_m passes through the centimeter band, after which we expect to see a decline similar to that seen in the optical ($f_\nu \propto t^{-2.2}$; Harrison et al. 1999). As can be seen from Figure 1, the radio observations are grossly inconsistent with these expectations; in particular, the decay is much faster than $t^{-1/3}$.

To summarize, while the optical and X-ray observations can be accounted for by a jet model, the radio observations are inconsistent with the standard model. This forces us to consider afterglow models in which some of the radio emission arises from a source other than the usual forward shock.

4. A FORWARD AND REVERSE SHOCK MODEL

The most natural explanation for two components would be an early contribution from a reverse shock followed by a forward shock element at later times. This is the explanation invoked to account for the early (1–2 day) radio emission from the afterglow of GRB 990123 (Sari & Piran 1999; Kulkarni et al. 1999). The two bursts share several common features. In both cases a jet was deduced with $t_j \sim$ a few days, both were quite bright at gamma-ray energies, and both had a seemingly small value of t_m (as measured in the centimeter band). However, in the case of GRB 990123, the peak flux of the forward shock was $f_m < 260$ μJy and the radio light curve was dominated by the reverse shock. In contrast, the forward shock for GRB 991216 appears to be quite strong. This difference then explains the seemingly different radio light curves.

At late times (i.e., timescales greater than the duration of the burst) the flux from the reverse shock is expected to fall as $t^{-1.8}$ (Kobayashi & Sari 1999). In contrast, the forward shock emission rises as $t^{1/2}$ for $t < t_j$ and then slowly decays, proportional to $t^{-1/3}$, until the ν_m moves into the centimeter band. Since t_j is known from optical observations (Halpern et al. 2000), the remaining unknowns are the strength of the reverse and forward shock emission.

In this picture, the reverse shock dominates the radio emission for the first few days, and the model fit mainly consists of fitting a power law with $f_\nu \propto t^{-1.8}$. We note that at day 1.5, the VLA 8.46 GHz flux and the Ryle 15 GHz flux are comparable. This suggests that the reverse shock is already optically thin at 8.46 GHz at this epoch—similar to the situation for GRB 990123 (Kulkarni et al. 1999). We deduce the parameters of the forward shock by fitting the radio to optical spectrum around $t_j = 5$ days to the forward shock model (the contribution of the reverse shock is expected to be negligible thanks to the steep decay, and since t is comparable to t_j the spherical fireball model is still applicable); we find $\nu_m \sim 1.4 \times 10^{12}$ Hz and $f_m = 1$ mJy. As can be seen from Figure 3 this reverse-forward model provides a reasonable fit to the observations.

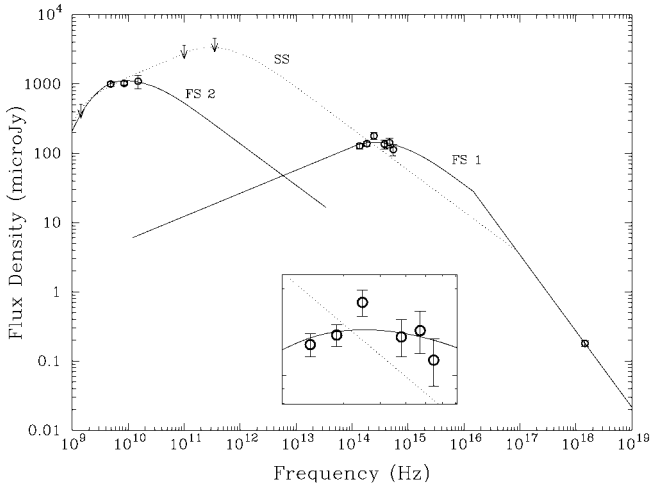

FIG. 2.—Radio to X-ray spectral flux distribution of GRB 991216 on 1999 December 18.00 ($\Delta t = 1.33$ days after the burst). Optical and infrared measurements are taken from Halpern et al. (2000). The optical/IR data have been corrected for Galactic foreground extinction (Schlegel, Finkbeiner, & Davis 1998), giving $E(B-V) = 0.634$ with an uncertainty of 10%. The 1.4 GHz upper limit (plotted as 3 times the rms noise) and the 4.8 GHz data point were taken at the Westerbork Synthesis Radio Telescope by Rol et al. (1999). The flux density at 8.46 GHz was derived by extrapolating the power-law decay in Fig. 1. The upper limits at 100 and 350 GHz have been extrapolated back to this epoch by assuming a worst case decay rate of $\alpha_o - 2\ \sigma$. The dotted and solid lines are fits to the data for a synchrotron spectrum from a relativistic blast wave as specified by Granot, Piran, & Sari (1999a; see their Fig. 10 for the equipartition field model). We assume $p = 2.2$ and scale it by ν_m and f_m to derive a function $g(\nu)$ with asymptotic limits of $\nu^{1/3}$ and $\nu^{(p-1)/2}$. We account for synchrotron self-absorption at ν_a by multiplying $g(\nu)$ by $F_\nu = [1 - \exp(-\tau)]/\tau$, where $\tau = (\nu/\nu_a)^{-5/3}$ (Granot, Piran, & Sari 1999b).

There are three predictions of this model. First, we expect ν_m to cross the centimeter band at $t_b = t_j(\nu_m/8.46\ \mathrm{GHz})^{1/2} \sim 64$ days. For $t > t_b$, we expect the radio flux to decline as steeply as the optical flux does for $t > t_j$. The low flux values as measured at the VLA around this epoch are in agreement with this model. A second prediction is that for $t < t_b$ the spectrum should rise as $\nu^{1/3}$ for $\nu < 8.46$ GHz. The observed radio slope between 1.43 and 8.46 GHz at day 17.44 can be described by a simple power law with slope $\beta_r = -0.39$ and agrees with the model prediction at the 90% confidence level (1.6 σ). Finally, within this interpretation, we expect there to have been an optical flash of approximately eighth magnitude.

5. A TWO-COMPONENT FORWARD SHOCK MODEL

We now consider a model in which much of the radio emission arises as the forward shock of an additional fireball (hereafter the second fireball). The principal attraction of the second fireball is that we no longer need to relate the radio decay rate to those at optical and radio frequencies. We clarify that the optical and X-ray observations are explained by the forward

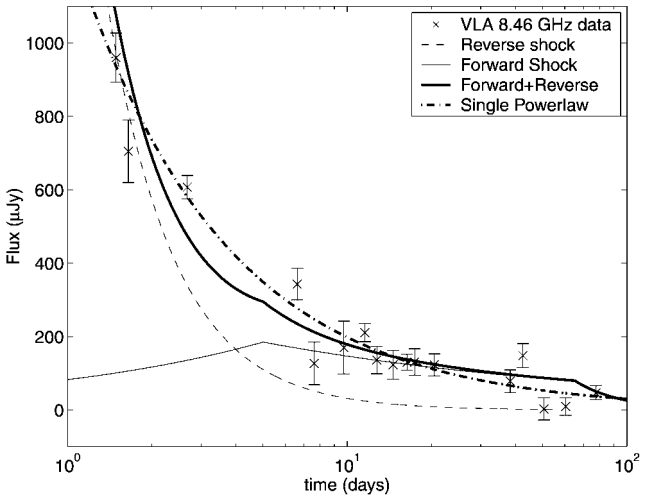

FIG. 3.—Observed and model light curves at 8.46 GHz. The dot-dashed line is the power-law fit from Fig. 1. The thick solid line is the two-component model discussed in § 4, consisting of a reverse shock (*dashed line*) and a forward shock (*thin solid line*). See text for more details.

shock of the first fireball (FS 1 in Fig. 2). As noted in § 3, there is good evidence suggesting that the first fireball is a jet. Thus, the second fireball must be a more isotropic fireball and move at a smaller Lorentz factor. Indeed, in some GRB models, the central engine is expected to inject two fireballs: a high-Γ jet and a low-Γ spherical wind (Panaitescu, Meszaros, & Rees 1998).

A reasonable fit to the radio data of this second fireball (FS 2; see Fig. 2) on day 1.33 is provided by $f_{m2} \simeq 1.2$ mJy, $\nu_{m2} = 7$ GHz, and $\nu_{a2} = 2$ GHz. The location of the cooling frequency ν_{c2} is unconstrained. As a test, we evolved the afterglow spectrum forward in time. While the model does an excellent job reproducing the declining flux density from 1.43 and 8.46 GHz at 17.44 days, at day 60.40 it predicts a 1.43 GHz flux of $\sim$270 μJy, where only an upper limit of -55 ± 37 μJy is measured. We consider this to be the weakest point of the model but do not consider it fatal since the quoted uncertainties include only instrumental errors and do not include external effects such as interstellar scintillation.

The three inferred parameters (ν_{m2}, f_{m2}, ν_{a2}) allow us to obtain the energy of the blast wave and the density of the ambient medium (Wijers & Galama 1999), $E_{52} \sim 10^2$ and $n \sim 10^{-4}$ cm^{-3}; these values are relatively insensitive to the value of the unknown ν_c (which is, however, constrained to lie above the optical band). The large E and small n are primarily due to the small value of t_m. If this interpretation is correct, then we have uncovered the first example of a GRB exploding in a very low density medium—perhaps the halo of a host galaxy.

We end this section by noting a worrisome and puzzling issue: we are unable to provide a consistent explanation for the near-IR, optical, and X-ray observations with a standard fireball afterglow spectrum. As noted in Figure 2, there is a broad maximum around 2×10^{14} Hz, suggesting that this is the peak frequency (ν_m) of the fireball. Fitting a template afterglow spectrum we obtain the following: $\nu_{m1} = 2.4 \pm 0.7 \times 10^{14}$ Hz, $f_{m1} = 144 \pm 10$ μJy, and $\nu_{c1} \simeq 2 \times 10^{16}$ Hz. A similar broad peak in the near-IR (and attributed to $\nu_m \sim 3 \times 10^{14}$ Hz at $\Delta t = 0.5$ days) was observed for GRB 971214 (Ramaprakash et al. 1998). However, if we evolve this ν_m back in time (with $\nu_m \propto t^{-3.2}$), we predict a *rising R*-band light curve, inconsistent with the observations (Fig. 1). Moving ν_m to lower frequencies solves this problem, but we are left with no explanation for the near-IR bump.

To summarize, the radio afterglow of GRB 991216 is unusual and cannot be explained by the standard forward shock model. A conventional reverse-forward shock model or an exotic two-component forward shock model can reasonably account for the observations. Finally, we have no explanation for the near-IR bump seen on day 1.33. GRB 991216 shows that there may yet be new surprises in GRB afterglows.

D. A. F. thanks C. Fassnacht, S. Myers, L. Yan, and J. Ulvestad for generously giving up portions of their VLA time so that GRB 991216 could be observed; J. Halpern for making his paper available prior to publication; and Y. Gallant and M. Vietri for useful discussions. We would like to thank S. Jogee for preparing the first observations of this burst at OVRO and A. Sargent for generously allocating the time on short notice. Research at OVRO is supported by the National Science Foundation through NSF grant AST 96-13717. S. R. K.'s research is supported by grants from NSF and NASA. R. S. and T. G. are supported by Sherman Fairchild Fellowships.

REFERENCES

Chevalier, R. A., & Li, Z.-Y. 1999, ApJ, 520, L29
Corbet, R., & Smith, D. 1999, GCN Circ. 506 (http://gcn.gsfc.nasa.gov/gcn/gcn3/506.gcn3)
Frail, D. A., Waxman, E., & Kulkarni, S. R. 2000, ApJ, 537, 191
Fukugita, M., Shimasaku, K., & Ichikawa, T. 1995, PASP, 107, 945
Granot, J., Piran, T., & Sari, R. 1999a, ApJ, 513, 679
———. 1999b, ApJ, 527, 236
Halpern, J. P., et al. 2000, ApJ, in press (astro-ph/0006206)
Harrison, F. A., et al. 1999, ApJ, 523, L121
Holland, W. S., et al. 1999, MNRAS, 303, 659
Kippen, R. M., Preece, R. D., & Giblin, T. 1999, GCN Circ. 463 (http://gcn.gsfc.nasa.gov/gcn/gcn3/463.gcn3)
Kobayashi, S., & Sari, R. 1999, preprint (astro-ph/9910241)
Kulkarni, S. R., et al. 1999, ApJ, 522, L97
Panaitescu, A., Meszaros, P., & Rees, M. J. 1998, ApJ, 503, 314
Piro, L., Garmire, G., Garcia, M., Marshall, F., & Takeshima, T. 1999, GCN Circ. 500 (http://gcn.gsfc.nasa.gov/gcn/gcn3/5000.gcn3)
Ramaprakash, A. N., et al. 1998, Nature, 393, 43
Rhoads, J. E. 1997, ApJ, 487, L1
Rol, E., Vreeswijk, P. M., Strom, R., Kouveliotou, C., Pian, E., Castro-Tirado, A., Hjorth, J., & Greiner, J. 1999, GCN Circ. 491 (http://gcn.gsfc.nasa.gov/gcn/gcn3/491.gcn3)
Sari, R., & Piran, T. 1999, ApJ, 517, L109
Sari, R., Piran, T., & Halpern, J. P. 1999, ApJ, 519, L17
Sari, R., Piran, T., & Narayan, R. 1998, ApJ, 497, L17
Schlegel, D. J., Finkbeiner, D. P., & Davis, M. 1998, ApJ, 500, 525
Shepherd, D. S., Frail, D. A., Kulkarni, S. R., & Metzger, M. R. 1998, ApJ, 497, 859
Takeshima, T., Markwardt, C., Marshall, F., Giblin, T., & Kippen, R. M. 1999, GCN Circ. 478 (http://gcn.gsfc.nasa.gov/gcn/gcn3/478.gcn3)
Taylor, G. B., & Berger, E. 1999, GCN Circ. 483 (http://gcn.gsfc.nasa.gov/gcn/gcn3/483.gcn3)
Uglesich, R., Mirabal, N., Halpern, J., Kassin, S., & Novati, S. 1999, GCN Circ. 472 (http://gcn.gsfc.nasa.gov/gcn/gcn3/472.gcn3)
Vreeswijk, P. M., et al. 1999, GCN Circ. 496 (http://gcn.gsfc.nasa.gov/gcn/gcn3/496.gcn3)
Wijers, R. A. M. J., & Galama, T. J. 1999, ApJ, 523, 177